Rotational Spectrum of Aminoborane: Centrifugal Distortion Constants and Boron and Nitrogen Hyperfine Structure

Kirsten Vormann, Helmut Dreizler, Jens Doose, and Antonio Guarnieri
Abteilung Chemische Physik im Institut für Physikalische Chemie der Universität Kiel

Z. Naturforsch. **46 a,** 770–776 (1991); received June 22, 1991

The boron and nitrogen hyperfine structure in the rotational spectra of two aminoborane isotopomers, $^{11}BH_2NH_2$ and $^{10}BH_2NH_2$, has been investigated and the quadrupole coupling constants of boron ^{10}B, ^{11}B and nitrogen ^{14}N have been determined. We get the following results for the nuclear quadrupole coupling constants: $\chi_{aa}(^{11}B) = -1.684\,(14)$ MHz, $\chi_{bb}(^{11}B) = -2.212\,(11)$ MHz, $\chi_{cc}(^{11}B) = 3.896\,(11)$ MHz, $\chi_{aa}(^{10}B) = -3.481\,(11)$ MHz, $\chi_{bb}(^{10}B) = -4.623\,(14)$ MHz, $\chi_{cc}(^{10}B) = 8.104\,(14)$ MHz and $\chi_{aa}(^{14}N) = 0.095\,(9)$ MHz, $\chi_{bb}(^{14}N) = 2.091\,(8)$ MHz, $\chi_{cc}(^{14}N) = -2.186\,(8)$ MHz. These nitrogen quadrupole coupling constants are those of the $^{11}BH_2{}^{14}NH_2$ isotopomer. Additionally we were able to determine two out of the three spin rotation coupling constants c_{aa}, c_{bb}, and c_{cc} of boron, $c_{aa}(^{11}B = 55.2\,(26)$ kHz, $c_{bb}(^{11}B) = 6.62\,(36)$ kHz, $c_{aa}(^{10}B) = 15.26\,(69)$ kHz and $c_{bb}(^{10}B) = 4.94\,(70)$ kHz. The spin rotation coupling constants c_{cc} had to be fixed to zero in both cases. Furthermore we measured the rotational spectra in the mm-wave region to determine all quartic and several sextic centrifugal distortion constants according to Watson's A and S reduction.

Key words: Microwave spectroscopy; Centrifugal distortion constants; Nuclear quadrupole hyperfine structure, Aminoborane.

Introduction

Aminoborane, BH_2NH_2, belongs to the isoelectronic inorganic analogs of simple hydrocarbons, where pairs of carbon atoms are replaced by boron and nitrogen. In general the BN-analogs are less stable than the hydrocarbons; aminoborane, e.g., polymerizes very quickly at room temperature and normal pressures whereas ethylene is stable under these conditions. Therefore it is difficult to study BH_2NH_2 in the gas phase.

The rotational and centrifugal distortion constants of five isotopomers of aminoborane, $^{11}BH_2{}^{14}NH_2$, $^{10}BH_2{}^{14}NH_2$, $^{11}BH_2{}^{15}NH_2$, $^{11}BD_2{}^{14}NH_2$, and $^{11}BH_2{}^{14}ND_2$ were first determined by Sugie, Takeo and Matsumura [1]. Using these rotational constants, they calculated the complete r_s structure of the unstable molecule. Some of the transitions they observed, showed a hyperfine pattern due to the quadrupole coupling of boron and nitrogen. They were not able to determine all quadrupole coupling constants from these transitions. The χ_{aa} coupling constants of both nuclei (^{11}B and ^{14}N) were fixed to values, calculated with the aid of ab initio molecular orbital methods.

Experimental

The substance was prepared by controlled thermal decomposition of borane-ammonia, BH_3NH_3, to aminoborane in a flow system.

$$BH_3NH_3 \xrightarrow{360\,K} BH_2NH_2 + H_2 .$$

This preparation method was first used by Gerry et al. [2], who studied the infrared spectrum of the substance.

The borane-ammonia BH_3NH_3 was obtained commercially from Fa. Alfa Products, Karlsruhe, and used without further purification. The lifetime of the BH_2NH_2 was about 10 min in the brass cells of the microwave Fourier transform (MWFT) spectrometers [3–6] and about 60 min after conditioning in the glass cell of the millimeter-wave spectrometer [7]. The high resolution spectra of the different isotopomers up to 40 GHz where recorded with microwave Fourier transform spectrometers at a temperature of 223 K and pressures between 0.13 and 0.65 Pa. All rotational transitions which were used for the hyperfine structure

---

Reprint requests to Prof. Dr. H. Dreizler, Institut für Physikalische Chemie der Universität Kiel, Olshausenstr. 40–60, D-2300 Kiel.

0932-0784 / 91 / 0900-0770 $ 01.30/0. – Please order a reprint rather than making your own copy

Table 1 a. Rotational transitions of $^{11}BH_2{}^{14}NH_2$. ν_c: hypothetical center frequency, ν_{obs}: frequency of the hyperfine component, $\Delta\nu_{exp}$: experimental hfs-splitting referred to the hypothetical center frequency, $\Delta\nu_{calc}$: calculated hfs-splitting referred to the center frequency, δ: difference between experimental and calculated hfs-splitting. The transition $J K_- K_+ - J' K'_- K'_+ = 1_{01} - 0_{00}$, marked with *, is not included in the hfs-analysis.

$J K_- K_+ - J' K'_- K'_+$				ν_c [MHz]			
F	I	F'	I'	ν_{obs} [MHz]	$\Delta\nu_{exp}$ [MHz]	$\Delta\nu_{calc}$ [MHz]	δ [MHz]
$1_{01} - 0_{00}$*				50366.018			
0.5	0.5	0.5	0.5	50365.666	−0.353	−0.321	−0.032
0.5	1.5	0.5	0.5	50366.452	0.433	0.413	0.020
1.5	0.5	0.5	0.5	50366.112	0.093	0.075	0.018
0.5	0.5	1.5	1.5	50365.666	−0.353	−0.321	−0.032
0.5	1.5	1.5	1.5	50366.452	0.433	0.413	0.020
1.5	1.5	1.5	1.5	50365.666	−0.353	−0.357	0.004
1.5	2.5	1.5	1.5	50366.452	0.433	0.415	0.019
2.5	1.5	1.5	1.5	50366.112	0.093	0.105	−0.012
2.5	2.5	1.5	1.5	50365.666	−0.353	−0.337	−0.016
1.5	1.5	2.5	2.5	50365.666	−0.353	−0.357	0.004
1.5	2.5	2.5	2.5	50366.452	0.433	0.415	0.019
2.5	1.5	2.5	2.5	50366.112	0.093	0.105	−0.012
2.5	2.5	2.5	2.5	50365.666	−0.353	−0.337	−0.016
3.5	2.5	2.5	2.5	50366.112	0.093	0.084	0.009
$1_{10} - 1_{11}$				4608.382			
0.5	1.5	0.5	0.5	4607.406	−0.976	−0.954	−0.022
1.5	0.5	0.5	0.5	4608.591	0.209	0.226	−0.017
1.5	1.5	0.5	1.5	4609.205	0.823	0.831	−0.008
1.5	2.5	0.5	1.5	4606.518	−1.864	−1.856	−0.008
0.5	1.5	1.5	0.5	4607.406	−0.976	−0.981	0.005
0.5	0.5	1.5	1.5	4609.922	1.540	1.529	0.011
0.5	1.5	1.5	1.5	4608.474	0.092	0.082	0.010
0.5	0.5	1.5	2.5	4607.905	−0.477	−0.474	−0.003
1.5	0.5	1.5	0.5	4608.591	0.209	0.199	0.010
1.5	2.5	1.5	1.5	4608.292	−0.090	−0.108	0.018
1.5	0.5	1.5	2.5	4607.638	−0.744	−0.741	−0.003
1.5	1.5	1.5	2.5	4608.952	0.570	0.575	−0.005
2.5	1.5	1.5	1.5	4608.979	0.597	0.605	−0.008
2.5	2.5	1.5	2.5	4608.292	−0.090	−0.094	0.004
1.5	1.5	2.5	1.5	4609.205	0.823	0.830	−0.007
1.5	2.5	2.5	2.5	4607.569	−0.813	−0.812	−0.001
2.5	1.5	2.5	1.5	4607.240	−1.142	−1.144	0.002
2.5	1.5	2.5	2.5	4608.292	−0.090	−0.099	0.009
2.5	2.5	2.5	2.5	4609.592	1.210	1.206	0.004
3.5	2.5	2.5	1.5	4607.772	−0.610	−0.612	0.002
3.5	2.5	2.5	2.5	4608.809	0.427	0.433	−0.006
2.5	1.5	3.5	2.5	4607.756	−0.626	−0.619	−0.007
2.5	2.5	3.5	2.5	4609.073	0.691	0.687	0.004
3.5	2.5	3.5	2.5	4608.292	−0.090	−0.087	−0.003
$2_{11} - 2_{12}$				13824.728			
0.5	2.5	0.5	1.5	13823.814	−0.914	−0.906	−0.008
1.5	2.5	0.5	1.5	13822.784	−1.944	−1.948	0.004
1.5	1.5	0.5	2.5	13825.774	1.046	1.055	−0.009
0.5	1.5	1.5	2.5	13822.784	−1.944	−1.951	0.007
1.5	0.5	1.5	0.5	13824.517	−0.211	−0.198	−0.013
1.5	1.5	1.5	1.5	13826.563	1.835	1.840	−0.005
2.5	1.5	1.5	1.5	13826.365	1.637	1.640	−0.003
1.5	2.5	2.5	0.5	13824.161	−0.567	−0.559	−0.008
1.5	1.5	2.5	1.5	13826.242	1.514	1.525	−0.011
1.5	2.5	2.5	2.5	13823.578	−1.150	−1.155	0.005
2.5	0.5	2.5	0.5	13825.141	0.413	0.411	0.002
2.5	1.5	2.5	1.5	13826.031	1.303	1.325	−0.022
2.5	2.5	2.5	2.5	13823.957	−0.771	−0.778	0.007
3.5	2.5	2.5	0.5	13825.437	0.709	0.708	0.001
3.5	1.5	2.5	1.5	13824.877	0.149	0.151	−0.002
3.5	2.5	2.5	2.5	13824.834	0.106	0.112	−0.006
2.5	1.5	3.5	1.5	13824.517	−0.211	−0.218	0.007
2.5	0.5	3.5	2.5	13825.719	0.991	0.994	−0.003
2.5	2.5	3.5	2.5	13825.141	0.413	0.400	0.013
3.5	1.5	3.5	1.5	13823.338	−1.390	−1.391	0.001
3.5	2.5	3.5	2.5	13826.031	1.303	1.290	0.013
4.5	2.5	3.5	1.5	13823.957	−0.771	−0.762	−0.009
4.5	2.5	3.5	2.5	13825.563	0.835	0.828	0.007
3.5	1.5	4.5	2.5	13823.957	−0.771	−0.750	−0.021
3.5	2.5	4.5	2.5	13825.071	0.343	0.342	0.001
4.5	2.5	4.5	2.5	13824.606	−0.122	−0.121	−0.001
$3_{12} - 3_{13}$				27645.532			
1.5	1.5	1.5	1.5	27643.394	−2.138	−2.136	−0.002
1.5	2.5	1.5	2.5	27646.527	0.995	0.975	0.020
2.5	1.5	1.5	2.5	27646.774	1.242	1.238	0.004
1.5	2.5	2.5	1.5	27647.019	1.487	1.506	−0.019
2.5	0.5	2.5	0.5	27645.388	−0.144	−0.165	0.021
2.5	1.5	2.5	1.5	27647.288	1.756	1.769	−0.013
2.5	2.5	2.5	2.5	27644.140	−1.392	−1.391	−0.001
3.5	1.5	2.5	1.5	27647.019	1.487	1.491	−0.004
3.5	2.5	3.5	0.5	27644.951	−0.581	−0.585	0.004
3.5	0.5	3.5	1.5	27646.405	0.873	0.866	0.007
3.5	1.5	3.5	1.5	27646.527	0.995	1.005	−0.010
3.5	0.5	3.5	2.5	27646.074	0.542	0.540	0.002
4.5	1.5	4.5	1.5	27644.026	−1.506	−1.503	−0.003
4.5	2.5	4.5	2.5	27646.844	1.312	1.315	−0.003
5.5	2.5	5.5	2.5	27645.388	−0.144	−0.138	−0.006
$5_{23} - 5_{24}$				4878.239			
2.5	2.5	2.5	2.5	4878.193	−0.046	−0.045	−0.001
3.5	1.5	3.5	1.5	4877.949	−0.290	−0.292	0.002
3.5	2.5	3.5	2.5	4878.404	0.165	0.167	−0.002
4.5	2.5	4.5	0.5	4878.167	−0.072	−0.074	0.002
4.5	1.5	4.5	1.5	4878.465	0.226	0.227	−0.001
4.5	0.5	4.5	2.5	4878.147	−0.092	−0.090	−0.002
5.5	0.5	5.5	0.5	4878.251	0.012	0.015	−0.003
5.5	1.5	5.5	1.5	4878.369	0.130	0.132	−0.002
5.5	2.5	5.5	2.5	4878.219	−0.020	−0.019	−0.001
6.5	1.5	6.5	1.5	4878.079	−0.160	−0.171	0.011
6.5	2.5	6.5	1.5	4877.998	−0.241	−0.242	0.001
6.5	1.5	6.5	2.5	4878.441	0.202	0.202	0.000
6.5	2.5	6.5	2.5	4878.369	0.130	0.131	−0.001
7.5	2.5	7.5	2.5	4878.219	−0.020	−0.021	0.001
$6_{24} - 6_{25}$				9662.538			
3.5	2.5	3.5	2.5	9662.482	−0.056	−0.061	0.005
4.5	1.5	4.5	1.5	9662.137	−0.401	−0.401	0.000
4.5	2.5	4.5	2.5	9662.772	0.234	0.236	−0.002
5.5	2.5	5.5	0.5	9662.435	−0.103	−0.099	−0.004
5.5	1.5	5.5	1.5	9662.846	0.308	0.309	−0.001
5.5	0.5	5.5	2.5	9662.435	−0.103	−0.113	0.010
6.5	0.5	6.5	0.5	9662.549	0.011	0.014	−0.003
6.5	1.5	6.5	1.5	9662.734	0.196	0.194	0.002
6.5	2.5	6.5	2.5	9662.508	−0.030	−0.030	0.000
7.5	2.5	7.5	1.5	9662.207	−0.331	0.327	−0.004
7.5	1.5	7.5	2.5	9662.804	0.266	0.266	−0.000
8.5	2.5	8.5	2.5	9662.508	−0.030	−0.030	0.000
$7_{25} - 7_{26}$				17137.773			
4.5	2.5	4.5	2.5	17137.691	−0.082	−0.079	−0.003

Table 1 a. (Continued).

$J K_- K_+ - J' K'_- K'_+$				ν_c [MHz]			
F	I	F'	I'	ν_{obs} [MHz]	$\Delta\nu_{exp}$ [MHz]	$\Delta\nu_{calc}$ [MHz]	δ [MHz]
5.5	1.5	5.5	1.5	17 137.256	−0.517	−0.519	0.002
5.5	2.5	5.5	2.5	17 138.088	0.315	0.311	0.004
6.5	0.5	6.5	0.5	17 137.645	−0.128	−0.136	0.008
6.5	1.5	6.5	1.5	17 138.166	0.393	0.397	−0.004
6.5	2.5	6.5	2.5	17 137.645	−0.128	−0.126	−0.002
7.5	0.5	7.5	0.5	17 137.781	0.008	0.012	−0.004
7.5	1.5	7.5	1.5	17 138.038	0.265	0.263	0.002
7.5	2.5	7.5	2.5	17 137.732	−0.041	−0.044	0.003
8.5	2.5	8.5	1.5	17 137.345	−0.428	−0.428	−0.000
8.5	1.5	8.5	2.5	17 138.112	0.339	0.344	−0.005
9.5	2.5	9.5	2.5	17 137.732	−0.041	−0.040	−0.001
11_{29} – 12_{012}				34 312.802			
8.5	2.5	9.5	2.5	34 312.468	−0.334	−0.332	−0.002
9.5	1.5	10.5	1.5	34 310.887	−1.915	−1.907	−0.008
9.5	2.5	10.5	2.5	34 313.968	1.166	1.170	−0.004
10.5	0.5	11.5	0.5	34 312.750	−0.052	−0.071	0.019
10.5	2.5	11.5	0.5	34 312.413	−0.389	−0.380	−0.009
10.5	1.5	11.5	1.5	34 314.200	1.398	1.403	−0.005
10.5	0.5	11.5	2.5	34 312.329	−0.473	−0.480	0.007
11.5	0.5	12.5	0.5	34 312.750	−0.052	−0.047	−0.005
11.5	1.5	12.5	1.5	34 313.857	1.055	1.063	−0.008
11.5	2.5	12.5	2.5	34 312.663	−0.139	−0.151	0.012
12.5	1.5	13.5	1.5	34 311.206	−1.596	−1.587	−0.009
12.5	2.5	13.5	2.5	34 314.093	1.291	1.274	0.017
13.5	2.5	14.5	2.5	34312.663	−0.139	−0.136	−0.003

Table 1 b. Rotational transition of $^{10}BH_2{}^{14}NH_2$. All symbols are used in the same way as in Table 1 a.

$J K_- K_+ - J' K'_- K'_+$				ν_c [MHz]			
F	I	F'	I'	ν_{obs} [MHz]	$\Delta\nu_{exp}$ [MHz]	$\Delta\nu_{calc}$ [MHz]	δ [MHz]
1_{10} – 1_{11}				4898.517			
1	2	1	2	4897.194	−1.322	−1.323	0.001
2	2	1	2	4899.011	0.495	0.504	−0.011
1	2	2	2	4898.080	−0.436	−0.436	0.000
2	3	2	3	4896.632	−1.884	−1.877	−0.007
3	2	2	2	4899.011	0.495	0.493	0.002
3	3	2	3	4899.580	1.064	1.064	0.000
2	2	3	2	4899.580	1.064	1.068	−0.004
2	3	3	2	4897.492	−1.024	−1.025	0.001
2	3	3	3	4898.679	0.163	0.156	0.007
2	2	3	4	4898.521	0.005	0.006	−0.001
3	2	3	2	4898.679	0.163	0.169	−0.006
3	4	3	2	4897.332	−1.184	−1.179	−0.005
3	4	3	3	4898.521	0.005	0.001	0.004
3	2	3	4	4897.632	−0.884	−0.893	0.009
4	4	3	2	4899.793	1.277	1.268	0.009
4	3	3	3	4899.110	0.594	0.593	0.001
4	4	3	4	4898.727	0.211	0.206	0.005
3	3	4	3	4899.668	1.152	1.153	−0.001
3	2	4	4	4899.185	0.669	0.670	−0.004
3	4	4	4	4897.841	−0.675	−0.675	0.000
4	3	4	3	4897.164	−1.352	−1.350	−0.002
4	3	4	4	4898.431	−0.085	−0.084	−0.001
4	4	4	4	4900.282	1.766	1.773	−0.007
5	4	4	3	4897.632	−0.884	−0.884	0.000
5	4	4	4	4898.899	0.383	0.382	0.001
4	3	5	4	4897.632	−0.884	−0.881	−0.003
4	4	5	4	4899.492	0.976	0.975	0.001
5	4	5	4	4898.100	−0.416	−0.415	−0.001
2	2	3	3	4900.770	2.254	2.249	0.005
3	4	3	4	4896.280	−2.236	−2.242	0.006

Table 1 c. Rotational transition of $^{11}BH_2{}^{15}NH_2$. All symbols are used in the same way as in Table 1 a.

$J K_- K_+ - J' K'_- K'_+$		ν_c [MHz]			
F	F'	ν_{obs} [MHz]	$\Delta\nu_{exp}$ [MHz]	$\Delta\nu_{calc}$ [MHz]	δ [MHz]
6_{24} – 6_{25}		8944.572			
4.5	4.5	8944.378	−0.194	−0.193	−0.001
5.5	5.5	8944.675	0.103	0.104	−0.001
6.5	6.5	8944.751	0.179	0.178	0.001
7.5	7.5	8944.460	−0.112	−0.113	0.001

analysis of both nuclei, boron and nitrogen, are listed in Tables 1 a–c. The frequencies of all hyperfine components were determined by a least squares fit in the time domain to minimize overlapping effects in the frequency domain [8, 9]. The transitions above 40 GHz were recorded using a millimeter wave spectrometer with source modulation technique [7] at room temperature and pressures between 1 and 4 Pa.

The center frequencies of all rotational transitions of $^{11}BH_2{}^{14}NH_2$ which were used for the centrifugal distortion analysis are listed in Table 2. This Table contains also transitions given in [1].

Assignment of the Nuclear Hyperfine Structure

First calculations of the nuclear hyperfine structure of the rotational transitions were made using the rotational constants and the quadrupole coupling constants given in [2]. Comparison of the measured hyperfine pattern of the rotational transition $J K_- K_+ - J' K'_- K'_+ = 5 2 3 - 5 2 4$ with the corresponding calculated pattern shows that the coupling constants of [1] do not satisfactorily reproduce the hyperfine structure, see Figure 1.

After several attempts to assign the hyperfine structure of the transitions we chose the following way, which was finally successfull:

1. The measured rotational transition $J K_- K_+ - J' K'_- K'_+ = 1 0 1 - 0 0 0$ of $^{11}BH_2{}^{14}NH_2$ showed a

Table 2. Center frequencies of the rotational transitions of the isotopomer $^{11}BH_2{}^{14}NH_2$. $v_{c,\,calc}$: calculated center frequencies from Watson's S reduction, $v_{c,\,obs}$: hypothetical center frequency, δ: difference between calculated and hypothetical center frequency. Transitions marked with * are taken from [1].

$J K_- K_+ - J' K'_- K'_+$						$v_{c,\,calc}$ [MHz]	$v_{c,\,obs}$ [MHz]	δ [kHz]
1	0	1	0	0	0	50 365.922	50 366.022	−100
2	0	2	1	0	1	100 589.941	100 589.943	−2
2	1	2	1	1	1	96 121.387	96 121.415	−28
3	1	2	2	1	1	157 914.041	157 914.096	−55
3	2	1	2	2	0	151 648.481	151 648.496	−15
3	2	2	2	2	1	151 086.230	151 086.266	−36
3	0	3	2	0	2	150 531.079	150 531.054	25
4	0	4	3	0	3	200 052.835	200 052.827	8
4	2	3	3	2	2	201 334.044	201 334.062	−18
4	3	2	3	3	1	201 704.526	201 704.576	−50
4	3	1	3	3	0	201 720.640	201 720.611	29
4	2	2	3	2	1	202 733.761	202 733.780	−19
4	1	3	3	1	2	210 375.564	210 375.578	−14
5	0	5	4	0	4	249 031.606	249 031.538	68
5	2	4	4	2	3	251 484.063	251 484.017	46
5	3	3	4	3	2	252 237.005	252 237.016	−11
5	3	2	4	3	1	252 293.319	252 293.325	−6
5	2	3	4	2	2	254 259.537	254 259.495	42
5	1	5	4	1	4	239 700.420	239 700.402	18
5	1	4	4	1	3	262 677.693	262 677.717	−24
6	0	6	5	0	5	297 370.867	297 370.886	−19
6	1	6	5	1	5	287 284.381	287 284.357	24
10	2	8	11	0	11	36 433.372	36 433.392	−20
11	2	9	12	0	12	34 312.823	34 312.802	22
1	1	0	1	1	1	4 608.372	4 608.382	−11
2	1	1	2	1	2	13 824.702	13 824.728	−26
3	1	2	3	1	3	27 645.475	27 645.532	−57
4	1	3	4	1	4*	46 058.713	46 058.660	53
5	2	3	5	2	4	4 878.235	4 878.239	−3
6	2	4	6	2	5	9 662.532	9 662.538	−6
7	2	5	7	2	6	17 137.760	17 137.773	−13
8	2	6	8	2	7*	27 973.593	27 973.640	−47
9	2	7	9	2	8	42 761.225	42 761.190	35
12	3	9	12	3	10	12 741.397	12 741.400	−3
13	2	11	13	2	12	148 220.981	148 221.000	−19
13	3	10	13	3	11*	19 977.005	19 977.020	−15
14	3	11	14	3	12	30 090.007	30 089.987	20
15	3	12	15	3	13*	43 715.702	43 715.650	52
17	4	13	17	4	14	8 033.672	8 033.666	6
18	4	14	18	4	15	12 389.049	12 389.043	6
19	4	15	19	4	16*	18 571.857	18 571.880	−23
20	4	16	20	4	17	27 114.746	27 114.730	16
21	4	17	21	4	18*	38 613.208	38 613.230	−22
24	4	20	24	4	21	97 050.046	97 050.054	−8
24	5	19	24	5	20*	10 617.740	10 617.740	0
25	5	20	25	5	21*	15 549.924	15 549.930	−6
26	5	21	26	5	22*	22 331.502	22 331.470	32
27	5	22	27	5	23*	31 471.060	31 471.060	0
28	5	23	28	5	24*	43 544.490	43 544.500	−10
30	6	24	30	6	25*	8 465.343	8 465.360	−17
30	5	25	30	5	26	79 000.653	79 000.647	6

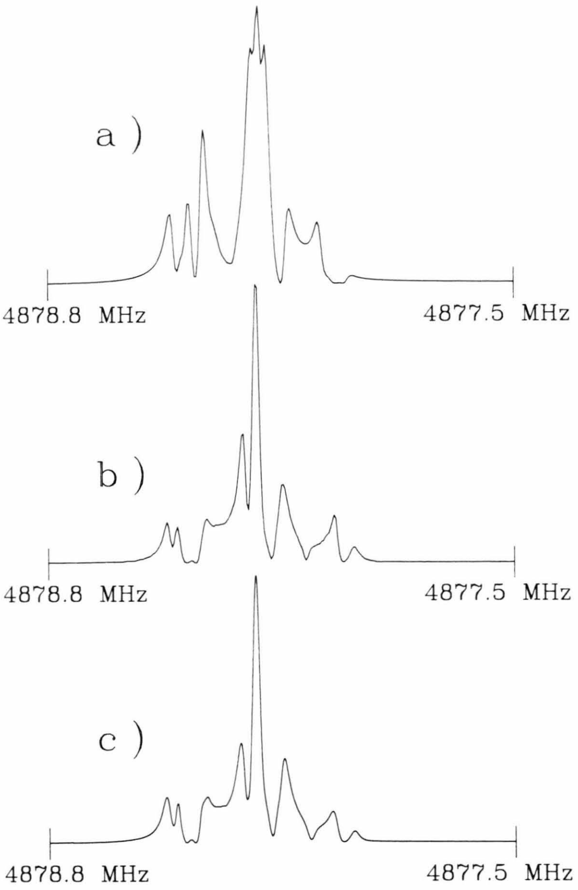

Fig. 1. The rotational transition $J K_- K_+ - J' K'_- K'_+ =$ 5 2 3 − 5 2 4 of the $^{11}BH_2{}^{14}NH_2$ isotopomer, a) power spectrum synthesized with the nuclear coupling constants given in [1], b) experimental power spectrum, polarizing frequency: 4877.0 MHz, sample interval: 50 ns, 2048 data points, $1.3 \cdot 10^6$ measuring cycles, 0.13 Pa, temperature: 223 K, c) power spectrum synthesized with our nuclear coupling constants.

triplet pattern. Theoretically, the hyperfine structure of this transition depends only on the χ_{aa} coupling constants of both nuclei. The triplet structure of the transition leads to the conclusion that one of the nuclei possesses a large coupling constant χ_{aa} while the other one must have a very small χ_{aa}. We had to distinguish between two possibilities. First, the boron coupling constant χ_{aa} is large while the χ_{aa} constant of the nitrogen is rather small, this leads to the result $\chi_{aa}(^{11}B) = 1.75$ MHz in good agreement with the calculated value $\chi_{aa}(^{11}B) =$ 1.6 MHz of [1]. Second, the nitrogen coupling constant χ_{aa} is large while the χ_{aa} constant of the boron is rather small. This leads to the result $\chi_{aa}(^{14}N) = -1.09$ MHz. The corresponding coupling constant given in [1] is $\chi_{aa}(^{14}N) = -0.6$ MHz.

2. We succeeded in measuring the rotational transition $J\,K_-\,K_+ - J'\,K'_-\,K'_+ = 6\,2\,4 - 6\,2\,5$ of the $^{11}BH_2{}^{15}NH_2$ isotopomer in natural abundance, see Table 1c. The hyperfine structure of this transition depends in good approximation only on the linear combination of the ^{11}B coupling constants, $[\chi_{bb}(^{11}B) - \chi_{cc}(^{11}B)]$. The ^{15}N nucleus causes no quadrupole interaction. We calculate $[\chi_{bb}(^{11}B) - \chi_{cc}(^{11}B)] = -6.1$ MHz, which is also in good agreement with the value $[\chi_{bb}(^{11}B) - \chi_{cc}(^{11}B)] = -6.0$ MHz of [1]. The hyperfine pattern of this transition gave us also the first hint that boron spin rotation coupling had to be taken into account.
3. Finally we made the assumption that the linear combination of the nitrogen coupling constants $[\chi_{bb}(^{14}N) - \chi_{cc}(^{14}N)] = 3.8$ MHz of [1] is well determined. This decision was based on two arguments, first the value of the boron coupling constant $[\chi_{bb}(^{11}B) - \chi_{cc}(^{11}B)]$ of [1] is in good agreement with our corresponding constant as mentioned above, and second the two coupling constants $(\chi_{bb} - \chi_{cc})$ of both nuclei, ^{11}B and ^{14}N, were experimentally determined.

With these considerations we obtained reliable starting values for three out of four nuclear quadrupole coupling constants; only one coupling constant, namely χ_{aa} of ^{14}N, remained uncertain.

The hyperfine structure of the rotational transitions of the $^{10}BH_2{}^{14}NH_2$ isotopomere is even more complicated than the corresponding hyperfine pattern of ^{11}B due to the nuclear spin, $I = 3$, of ^{10}B. There was only one transition of $^{10}BH_2{}^{14}NH_2$ which was appropriate to fit the nuclear coupling constants while the hyperfine structures of all other transitions were not resolved in a satisfactory way.

Results and Discussion of the Centrifugal Distortion Analysis

Aminoborane is a near prolate asymmetric top rotor ($\varkappa = -0.92$) with the dipole moment vector along the *a*-axis of inertia. Our first calculations of the rotational transitions of $^{11}BH_2{}^{14}NH_2$ were based on the rotational and centrifugal distortion constants given in [1]. Due to the large rotational constants there exist only Q-branch transitions in the microwave range. Further calculations, which take into account the rotational parameters of [2], showed that there exist two P-branch transitions at 34 and 36 GHz, $J\,K_-\,K_+ - J'\,K'_-\,K'_+ = 11\,2\,9 - 12\,0\,12$ and $J\,K_-\,K_+ - J'\,K'_-\,K'_+ = 10\,2\,8 - 11\,0\,11$. These transitions are relatively weak due to the selection rule $\Delta K_- = 2$, but they are highly sensitive to the centrifugal distortion constants and especially to the rotational constant *A*. Knowledge of the hyperfine structure of these rotational transitions enabled us to unambiguously identify them and determine their center frequencies.

Using the set of rotational parameters based on the transitions in the microwave range, the prediction of transitions in the millimeter wave region was accurate enough to identify the measured lines.

For the final fit we included all our center frequencies and additionally the center frequencies listed in [1]. Using the planarity relations [10] we were able to determine the rotational constants, all quartic centrifugal distortion constants and three of the sextic centrifugal distortion constants according to Watson's A and S reduction [11]. The other sextic constants Φ_{KJ}, Φ_K, φ_J and φ_K, respectively H_{KJ}, H_K, h_1 and h_3 had to be fixed to zero for the fit. Due to the planarity relations, the sextic order constants Φ_J in case of Watson's A reduction and h_2 in case of the S reduction were constrained to the other centrifugal distortion constants. The results of this analysis are listed in Table 3.

We were not able to resolve the K-doublet transitions $5_{42} - 4_{41}$ and $5_{41} - 4_{40}$, although the prediction gave a splitting of about 300 kHz for the center frequencies. We could measure only one strong line at 252071.76 MHz due the overlapping of the hyperfine structure. Its frequency is exactly the averaged frequency of the two calculated transitions. Therefore it was not included in Table 2 and in the fit.

As expected, some of the obtained parameters in the Watson's A reduced fit show larger errors than in the symmetric reduction.

In case of $^{10}BH_2{}^{14}NH_2$ we were not able to determine experimental center frequencies of the rotational transitions due to the overlapping of the hyperfine components, as mentioned above. Therefore we did not perform a centrifugal distortion analysis but used the rotational and centrifugal distortion constants given in [1].

Table 3. Rotational and centrifugal distortion constants of $^{11}BH_2{}^{14}NH_2$, standard errors of the constants are given in brackets, Φ_{KJ}, Φ_K, φ_J, *and* φ_K are fixed to zero in case of Watson's A reduction, H_{KJ}, H_K, h_1, and h_3 are fixed to zero in case of Watson's S reduction. σ: standard deviation of the fit, N: number of rotational transitions. $K_{max}|^{*,*}|$: highest correlation coefficient, h_2 and Φ_J constrained by planarity relations.

Distortion constants from Watson's S reduction			A reduction		
A	138 221.39 (9)	MHz	A	138 221.38 (9)	MHz
B	27 487.267 (2)	MHz	B	27 487.889 (3)	MHz
C	22 878.827 (3)	MHz	C	22 878.220 (3)	MHz
D_J	43.07 (3)	kHz	Δ_J	46.22 (3)	kHz
D_{JK}	314.6 (3)	kHz	Δ_{JK}	295.8 (3)	kHz
D_K	2.58 (2)	MHz	Δ_K	2.59 (2)	MHz
d_1	−8.615 (3)	kHz	δ_J	8.621 (3)	kHz
d_2	−1.565 (3)	kHz	δ_K	307.2 (6)	kHz
H_J	−0.73 (3)	Hz	Φ_J	−0.56 (6)	Hz
H_{JK}	1.4 (6)	Hz	Φ_{JK}	0.7 (5)	Hz
[H_{KJ}	0.0	Hz]	[Φ_{KJ}	0.0	Hz]
[H_K	0.0	Hz]	[Φ_K	0.0	Hz]
[h_1	0.0	Hz]	[φ_J	0.0	Hz]
h_2	0.050 (3)	Hz	φ_{JK}	7.2 (6)	Hz
[h_3	0.0	Hz]	[φ_K	0.0	Hz]
$\varkappa$	−0.92009124		$\varkappa$	−0.92007035	
σ	35	kHz	σ	35	kHz
N	51		N	51	
$K_{max}\lvert D_K, d_2\rvert$	0.940		$K_{max}\lvert \Delta_{JK}, \varphi_{JK}\rvert$	0.944	

Results and Discussion of the Hyperfine Structure Analysis

The hyperfine structure of the rotational transitions of both isotopomers, $^{11}BH_2{}^{14}NH_2$ and $^{10}BH_2{}^{14}NH_2$, were analysed by first order perturbation theory [12]. In case of $^{11}BH_2{}^{14}NH_2$ we made use of all transitions given in Table 1a with exception of the rotational transition $J K_- K_+ - J' K'_- K'_+ = 1\,0\,1 - 0\,0\,0$. This transition was omitted because of the higher uncertainties of the frequency determination.

Table 4a. ^{11}B quadrupole and spin rotation coupling constants and ^{14}N quadrupole coupling constants of $^{11}BH_2{}^{14}NH_2$, the spin rotation coupling constant c_{cc} of ^{11}B was fixed to zero, standard errors given in brackets. σ: standard deviation, N: number of components, $K_{max}|^{*,*}|$: highest correlation coefficient.

Nitrogen, ^{14}N:		Boron, ^{11}B:		
χ_+	−0.095 (9) MHz	χ_+	1.684 (14)	MHz
χ_-	4.277 (7) MHz	χ_-	−6.107 (9)	MHz
χ_{aa}	0.095 (9) MHz	χ_{aa}	−1.684 (14)	MHz
χ_{bb}	2.091 (8) MHz	χ_{bb}	−2.212 (11)	MHz
χ_{cc}	−2.186 (8) MHz	χ_{cc}	3.896 (11)	MHz
		c_{aa}	0.0552 (26)	MHz
		c_{bb}	0.00662 (36)	MHz
		[c_{cc}	0.0	MHz]
		σ	0.008	MHz
		N	116	
		$K_{max}\lvert\chi_+(^{14}N), \chi_+(^{11}B)\rvert$	0.452	

Table 4b. ^{10}B quadrupole and spin rotation coupling constants and ^{14}N quadrupole coupling constants of $^{10}BH_2{}^{14}NH_2$, the spin rotation coupling constant c_{cc} of ^{10}B was fixed to zero, standard errors given in brackets. σ: standard deviation, N: number of components, $K_{max}|^{*,*}|$: highest correlation coefficient.

Nitrogen, ^{14}N:		Boron, ^{10}B:		
χ_+	−0.098 (7) MHz	χ_+	3.481 (11)	MHz
χ_-	4.276 (7) MHz	χ_-	−12.726 (16)	MHz
χ_{aa}	0.098 (7) MHz	χ_{aa}	−3.481 (11)	MHz
χ_{bb}	2.089 (7) MHz	χ_{bb}	−4.623 (14)	MHz
χ_{cc}	−2.187 (7) MHz	χ_{cc}	8.104 (14)	MHz
		c_{aa}	0.01526 (69)	MHz
		c_{bb}	0.00494 (70)	MHz
		[c_{cc}	0.0	MHz]
		σ	0.005	MHz
		N	30	
		$K_{max}\lvert\chi_+(^{14}N), \chi_+(^{11}B)\rvert$	0.600	

$Q(^{10}B)/Q(^{11}B) = \chi^-(^{10}B)/\chi^-(^{11}B) = 2.084\,(4)$

Table 5. ^{11}B quadrupole coupling constants [MHz] of some compounds similar to aminoborane.

Compound	χ_{aa}	χ_{bb}	χ_{cc}	Lit.
BH_2NH_2	−1.684 (14)	−2.212 (11)	3.896 (11)	this work
CH_3BF_2	−2.713 (21)	−0.695 (27)	3.408 (27)	[15]
HBF_2	−0.75 (9)	−2.585 (106)	3.335 (106)	[16]
$C_6H_5BF_2$	−2.589 (12)	−0.600 (15)	3.189 (15)	[17]
BF_2OH	−1.477 (5)	−1.195 (6)	2.672 (6)	[18]

For the analysis of the hyperfine structure in the spectra of $^{10}BH_2{}^{14}NH_2$ we used the transition $J K_- K_+ - J' K'_- K'_+ = 1\,1\,0 - 1\,1\,1$, which is listed in Table 1b. We were able to determine all nuclear quadrupole coupling constants of $^{11}BH_2{}^{14}NH_2$ and $^{10}BH_2{}^{14}NH_2$. Additionally we had to take into account the boron spin rotation interaction to achieve a satisfactory fit within the measuring accuracy of our spectrometers. In case of $^{11}BH_2{}^{14}NH_2$ all spin rotation coupling constants c_{aa}, c_{bb} and c_{cc} were calculated, but one of them, c_{cc}, was zero within the standard error. In case of $^{10}BH_2{}^{14}NH_2$ only two of the constants c_{aa} and c_{bb} could be determined. Therefore we decided to fix c_{cc} for both isotopomers to zero. The results of the analysis of the hyperfine structures are listed in Table 4a for $^{11}BH_2{}^{14}NH_2$ and in Table 4b for $^{10}BH_2{}^{14}NH_2$. In Table 5 we present the quadrupole coupling constants of some boron compounds similar to aminoborane. With the assumption that the bonding orbitals of boron are in all cases sp^2-hybrids, the orbital perpendicular to the sp^2-plane is a pure p-orbital. The unbalanced occupations of these p-orbitals, caused by back donation of π-electrons from the boron bonding partners [13], are described approximately by the coupling constants χ_{cc}. The quadrupole coupling constant by a single p-electron of boron is $eQq_{210} = -5.39$ MHz [14]. The molecules listed in Table 5 may be classified in three groups. Aminoborane is the only member of the first group. This molecule has only one bonding partner possessing π-electrons, namely the NH_2-group. Members of the second group are HBF_2 and CH_3BF_2, each of them possesses two bonding partners with π-electrons, the fluorine atoms. $C_6H_5BF_2$ and BF_2OH are members of the third group. In this group all three bonding partners have π-electrons. Consequently, in this picture the member of the first group, aminoborane, with only one π-donor, possesses the highest positive χ_{cc} value, i.e. the lowest occupation of the pure p-orbital. The χ_{cc} values of the members of the second group are less positive, caused by the bonding with two π-donors. The members of the third group, each of them possessing three π-donors, have the lowest χ_{cc} values. The unbalanced occupation of the pure p-orbital increases from the first to the third group.

Acknowledgement

We thank the members of our group for help and discussion, the Deutsche Forschungsgemeinschaft, the Land Schleswig-Holstein and the Fonds der Chemie for funds.

[1] M. Sugie, H. Takeo, and C. Matsumura, J. Mol. Spectrosc. **123,** 286 (1987).
[2] M. C. L. Gerry, W. Lewis-Bevan, A. J. Merer, and N. P. C. Westwood, J. Mol. Spectrosc. **110,** 153 (1985).
[3] G. Bestmann, H. Dreizler, H. Mäder, and U. Andresen, Z. Naturforsch. **35 a,** 392 (1980).
[4] G. Bestmann and H. Dreizler, Z. Naturforsch. **37 a,** 58 (1982).
[5] W. Stahl, G. Bestmann, H. Dreizler, U. Andresen, and R. Schwarz, Rev. Sci. Instrum. **56,** 1759 (1985).
[6] Ch. Keussen, N. Heineking, and H. Dreizler, Z. Naturforsch. **44 a,** 215 (1989).
[7] J. Doose, A. Guarnieri, W. Neustock, R. Schwarz, F. Winther, and F. Hegelund, Z. Naturforsch. **44 a,** 538 (1989).
[8] I. Merke and H. Dreizler, Z. Naturforsch. **43 a,** 196 (1988).
[9] J. Haekel and H. Mäder, Z. Naturforsch. **43 a,** 203 (1988).
[10] J. K. G. Watson, 'Aspects of Quartic and Sextic Centrifugal Effects on Rotational Energy Levels', in: Vibrational Spectra and Structure, J. R. Durig Ed., Elsevier, New York 1977, p. 73.
[11] loc. cit. [10], p. 37 and 40.
[12] W. Gordy and R. L. Cook, 'Microwave Molecular Spectra', J. Wiley & Sons, New York 1984, Chapter IX, p. 4.
[13] loc. cit. [12], p. 780.
[14] loc. cit. [12], Table 14.2, p. 737.
[15] L. Engelbrecht, Diss. 1975, Universität Kiel.
[16] N. P. C. Westwood, W. Lewis-Bevan, and M. C. L. Gerry, J. Mol. Spectrosc. **106,** 227 (1984).
[17] K. Vormann and H. Dreizler, Z. Naturforsch. **44 a,** 84 (1989).
[18] K. Vorman and H. Dreizler, Z. Naturforsch. **44 a,** 1191 (1989).